Binary Spectral Minutiae Representation with Multi-Sample Fusion For Fingerprint Recognition

Haiyun Xu and Raymond N.J. Veldhuis
Department of Electrical Engineering, University of Twente
PO Box 217, 7500AE Enschede, The Netherlands
{h.xu,r.n.j.veldhuis}@ewi.utwente.nl

ABSTRACT

Biometric fusion is the approach to improve the biometric system performance by combining multiple sources of biometric information. The binary spectral minutiae representation is a method to represent a fingerprint minutiae set as a fixed-length binary string. This binary representation has the advantages of a fast operation and a small template storage. It also enables the combination of a biometric system with template protection schemes that require a fixed-length feature vector as input. In this paper, based on the spectral minutiae representation algorithm, we investigate the multi-sample fusion algorithms at the feature-, score-, and decision-level respectively. Furthermore, we propose different schemes to mask out unreliable bits. The algorithms are evaluated on the FVC2000-DB2 database and showed promising results.

Categories and Subject Descriptors

H.4 [**Information Systems Applications**]: Miscellaneous

General Terms

Security

Keywords

Biometrics, fingerprint, template protection

1. INTRODUCTION

Recognition of persons by means of biometric characteristics is gaining importance due to the high security and user convenience. Among various biometric identifiers, such as face, signature and voice, fingerprint has one of the highest levels of distinctiveness and performance [11] and it is the most commonly used biometric modality. Most fingerprint recognition systems are based on the use of a minutiae set. However, the low comparison (or matching) speed is limiting its application to search large databases. At the same time, the increasing *privacy concerns* make minutiae template protection a crucial task. The spectral minutiae representation is a method to represent a minutiae set as a fixed-length feature vector, which is invariant to translation, and in which rotation and scaling become translations, so that they can be easily compensated for [18, 21, 20]. These characteristics enable the combination of fingerprint recognition systems with template protection schemes and allow for a fast minutiae-based matching as well.

In order to apply the spectral minutiae representation with a template protection scheme based on fuzzy commitment and helper data schemes, such as [7] and [16], we need to quantize the real-valued spectral minutiae features into binary strings. A fixed-length binary representation also has additional advantages such as small template storage and high matching speed. Based on the *complex spectral minutiae representation* (SMC) [21], the *Spectral Bits* binary spectral minutiae representation was proposed in [20] and showed promising results. Since the recognition performance is the most important factor for a biometric system, in this paper, we will investigate methods to improve the recognition performance by fusing multiple spectral minutiae representations.

Biometric fusion, also known as multibiometrics, is the approach to improve the biometric system performance by combining multiple sources of biometric information. Ross et al. [15] describe five scenarios that are possible to obtain multiple sources of information: (1) Multi-sensor systems, where the information from a single biometric characteristic is obtained from different sensors; (2) Multi-algorithm systems, where the same biometric data is processed using different algorithms; (3) Multi-instance systems, where multiple units of the same biometric characteristic (for example, the left and right index fingers) are combined; (4) Multi-sample systems, where a single sensor is used to acquire multiple impressions of the same biometric characteristic; (5) Multi-modal system, where different biometric characteristics (such as iris and fingerprint) from the same person are combined. Considering the cost effectiveness and user convenience, scenarios (1)(3)(5) may not be preferred. Scenario (2) is a popular cost-effective way to improve the biometric recognition performance. Prabhakar and Jain tried several attempts of combining multiple classifiers, and concluded that the improvement in recognition performance is closely related to the independence among various classifiers [12]. In this paper, we focus on the spectral minutiae algorithm and we will not involve other classifiers in this paper (for instance, a non-minutiae based classifier). Therefore, we will investigate scenario (4), fusing multiple enrollment samples, to improve the recognition performance.

Based on the difference in the level of available information, fusion strategies can be applied at image-level, feature-level, score-level and decision-level [11, 15]. In this paper, we focus on the procedures after the fingerprint minutiae extraction. Therefore, we will discuss the fusion strategies at feature-, score- and decision-level, respectively.

The main contributions of this paper are: (1) based on the method

MM&Sec'10, September 9–10, 2010, Roma, Italy.

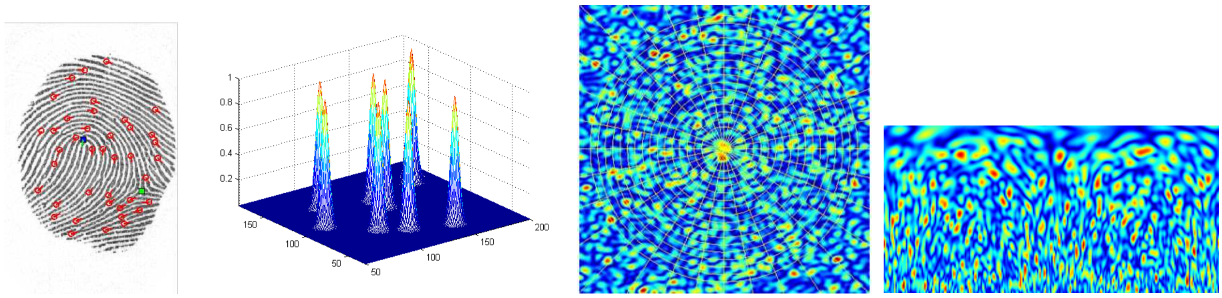

(a) (b) (c) (d)

Figure 1: Illustration of the complex spectral minutiae representation procedure. (a) a fingerprint and its minutiae; (b) representation of minutiae points as complex valued continuous functions; (c) the 2D Fourier spectrum of 'b' in a Cartesian coordinate and a polar sampling grid; (d) the Fourier spectrum sampled on a polar grid.

presented in [17], the minutiae quality data are incorporated to enhance the Complex Spectral Minutiae Representation (SMC) performance; (2) we investigate the multiple enrollment samples fusion at the feature-, score-, and decision-level respectively; (3) we investigate and evaluate several mask schemes, and discuss their application in context with template protection and error correction schemes.

In this paper, we will first present the *minutiae quality incorporated complex spectral minutiae representation* together with the *Column-PCA* feature reduction algorithm in Section 2. Next, in Section 3, we will briefly review the *Spectral Bits* quantization method, and propose several masks schemes. Then, in Section 4, we will discuss several methods to implement multi-sample fusions. Finally, we will show the experimental results in Section 5 and draw conclusions in Section 6.

2. COMPLEX SPECTRAL MINUTIAE REPRESENTATION

2.1 Minutiae Quality Incorporated Complex Spectral Minutiae Representation

The objective of the spectral minutiae representation is to represent a minutiae set as a fixed-length feature vector, which is invariant to translation and rotation [18]. We assume that the scaling has already been compensated for on the level of the minutiae sets. This is for instance possible if minutiae are presented in a standard like [1], which includes sensor resolution. In Figure 1, the procedure of the complex spectral minutiae representation (SMC) is illustrated.

Assume a fingerprint with Z minutiae. First, we code the minutiae locations by indicator functions, which are isotropic two-dimensional Gaussian kernels in the spatial domain. Then we incorporate the minutiae orientation by assigning each Gaussian a complex amplitude $\mathrm{e}^{\mathrm{j}\theta_i}, i = 1, \dots, Z$. In this way, we represent minutiae points as complex valued continuous functions, the magnitude of which is shown in Figure 1(b). In this representation, translation and rotation may exist, depending on how the user has put his finger on the sensor.

Next, a two-dimensional continuous Fourier transform is performed and only the Fourier magnitude is kept, illustrated in Figure 1(c). This representation is now translation invariant according to the shift property of the continuous Fourier transform. In addition, we incorporate the minutiae quality data as presented in [17] into SMC. This representation can be computed *analytically*,

$$\mathcal{M}_{\mathrm{C}}(\omega_{\mathrm{x}}, \omega_{\mathrm{y}}; \sigma_{\mathrm{C}}^2) = \left| \exp\left(-\frac{\omega_{\mathrm{x}}^2 + \omega_{\mathrm{y}}^2}{2\sigma_{\mathrm{C}}^{-2}}\right) \sum_{i=1}^{Z} w_i \exp(-\mathrm{j}(\omega_{\mathrm{x}} x_i + \omega_{\mathrm{y}} y_i) + \mathrm{j}\theta_i) \right|, \quad (1)$$

with $(x_i, y_i, \theta_i, w_i)$ the location, orientation and quality of the i-th minutia in the fingerprint, and $(\omega_{\mathrm{x}}, \omega_{\mathrm{y}}; \sigma_{\mathrm{C}}^2)$ are the frequencies and the parameters of the Gaussian kernel function respectively.

Finally, the Fourier spectrum is re-mapped onto a polar coordinate system, illustrated in Figure 1(d). In the radial direction λ, we use $M = 128$ samples between $\lambda_{\mathrm{l}} = 0.05$ and $\lambda_{\mathrm{h}} = 0.58$. In the angular direction β, we use $N = 256$ samples uniformly distributed between $\beta = 0$ and $\beta = 2\pi$. Since our target application is in a high security scenario with reasonable good quality fingerprints, we choose $\sigma_{\mathrm{C}} = 0$ for the best good performance. In this case, there is no multiplication with a Gaussian in the frequency domain (an analysis of the selection of the Gaussian parameter σ can be found in [18]). According to the rotation properties of the two-dimensional continuous Fourier transform, now the rotation becomes translation along the new coordinate axis.

2.2 Spectral Minutiae Matching

Let $R(m, n)$ and $T(m, n)$ be the two sampled minutiae spectra, respectively, achieved from the *reference* fingerprint and *test* fingerprint. Both $R(m, n)$ and $T(m, n)$ are normalized to have zero mean and unit energy. We use the two-dimensional correlation coefficient between R and T as a measure of their similarity.

In practice, the input fingerprint images are rotated. Therefore, we need to test a few rotations, which become the circular shifts in the horizontal direction. We denote $T(m, n-j)$ as a circularly shifted version of $T(m, n)$, the final matching score between R and T is,

$$S^{(R,T)} = \max_j \{ \frac{1}{MN} \sum_{m,n} R(m, n) T(m, n-j) \}, \quad -15 \leq j \leq 15. \quad (2)$$

2.3 Feature Reduction

The spectral minutiae feature is a 32,768-dimensional real-valued feature vector. This large dimensionality of the spectral minutiae feature can cause three problems. First, the template storage requirement is very high. Second, the high dimensionality leads to a computational burden and the matching speed will be limited.

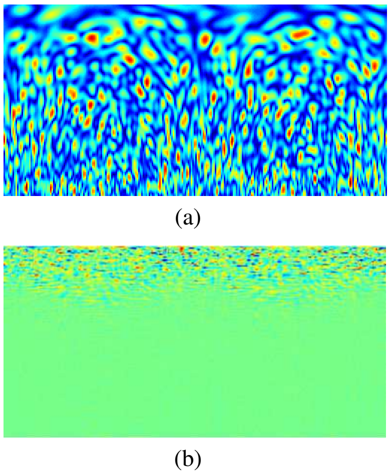

Figure 2: Illustration of the CPCA transform. (a) the SMC feature; (b) the minutiae spectrum after the CPCA transform.

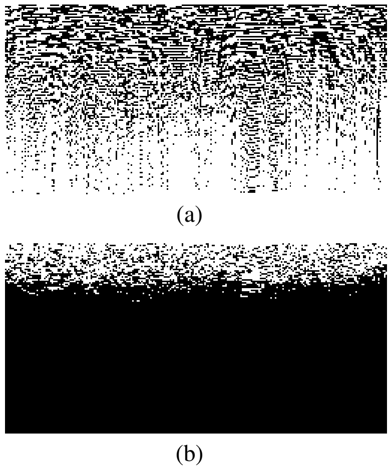

Figure 3: Example of Spectral Bits (SMC spectra after CPCA). (a) the Sign Bit; (b) the Mask Bit.

Third, the high dimensionality can lead to a small sample size problem [14]. In order to cope with these problems, we will apply the *Column Principal Component Analysis* (CPCA) feature reduction method introduced in [19].

The idea of CPCA is to apply the well known Principal Component Analysis (PCA) technique to the SMC columns. PCA has two functions: it decorrelates features and concentrates power. The CPCA representation is shown in Figure 2(b). We can see that after CPCA, the power is concentrated in the upper lines. The features in the lower parts are close to zero, so we can remove them from the representation. For the CPCA feature reduction, we keep the top 40 lines, with a feature reduction rate of 69%.

3. QUANTIZATION AND MASKING

3.1 Spectral Bits

In this section, we will first review the quantization method *Spectral Bits* introduced in [20]. The Spectral Bits quantization is applied to the real-valued features after the CPCA feature reduction. First, each real-valued feature is quantized as one bit (1 if the feature is greater than zero and 0 otherwise, we call it sign bit), shown in Figure 3(a). Second, since the quantization boundary is zero, and the features close to zero are unstable and likely to flip, they may cause errors. Therefore, we will mask out the features of which the absolute values are below a certain threshold. For the best recognition performance, we set the threshold to 0.6 after normalizing the spectra to have a standard deviation (STD) equal to 1. By testing different thresholds on different fingerprint databases, we found out that this parameter can be chosen empirically and it will not cause critical degradation of recognition performance. An example of the resulting mask bit is shown in Figure 3(b).

3.2 Fractional Hamming Distance (FHD)

After generating sign bit and mask bit vectors, we can compute a Fractional Hamming distance (FHD) [3] as a measure of the dissimilarity between two fingerprints spectra $R(m, n)$ and $T(m, n)$, whose sign bit vectors are denoted {codeR, codeT} and whose mask bit vectors are decoded {maskR, maskT},

$$FHD = \frac{||(\text{codeR} \otimes \text{codeT}) \cap \text{maskR} \cap \text{maskT}||}{||\text{maskR} \cap \text{maskT}||}. \quad (3)$$

3.3 FHD with Different Masks Schemes

As shown in Equation (3), we use the fractional Hamming Distance (FHD) as the similarity measure between two binary strings. This is the same measure applied for iris recognition by Daugman [3]. For a biometric verification system, we call maskR and maskT in Equation (3) the *enrollment mask* and *verification mask* respectively.

To combine a biometric system with template protection schemes based on fuzzy commitment and helper data schemes, such as [7] and [16], an *error correction scheme* [9] is needed to correct the bit errors. However, incorporating masks will introduce complexity to the error correction scheme, since at the time of encoding, only the enrollment mask is known, not the verification mask. For this reason, Hao et al. did not incorporate masks when applying template protection to iris recognition [5]. Bringer et al. proposed a method to enable masks by enhancing the fuzzy commitment scheme [2]. In this method, the error correction decoding also need to correct the masks errors.

Including masks in the similarity measurement can improve the recognition performance. To include masks, and at the same time, not to complicate the error correction and template protection scheme, we would like to investigate different mask schemes that can be easily incorporated to the error correction schemes.

In order to reach this target, we first impose several constraints on our mask schemes: (1) in case that an enrollment mask is used, the verification mask will be the same as the enrollment mask, and the number of masked components should be fixed to avoid the error correction coding difficulties. (2) In case that a verification mask will be used, we will not include enrollment mask. In this case, the verification mask can be incorporated by using erasure decoding.

Before presenting the mask schemes, we would like to introduce two components selection algorithms: *Largest Components Selection* (LCS) and *Reliable Components Selection* (RCS).

Largest Components Selection (LCS). LCS is a straightforward method that has been applied to the Spectral Bits mask selection. LCS will select the features with the largest absolute values. The features that are not chosen will be masked out.

Reliable Components Selection (RCS). To implement RCS, we need to estimate the within-class variance based on the multiple enrollment samples from the same subject [16]. Assume we have N_{E}

enrollment spectral minutiae representation samples, $R_1(m,n), \ldots, R_{N_{\mathrm{E}}}(m,n)$, $\mu_{m,n}$ and $\sigma^2_{m,n}$ are the mean and variance of each component at location (m,n). Since the spectral minutiae features in the same row is uniformly sampled (see Section 2), we assume that they have equal within-class variance. In this way, we can make a more reliable estimation of the within-class variance per line σ^2_m by average $\sigma^2_{m,n}$. Finally, the reliability factor $q_{m,n}$ of each component is calculated as

$$q_{m,n} = \frac{|\mu_{m,n}|}{\sigma_m}, \tag{4}$$

and the components with largest $q_{m,n}$ will be selected in the RCS scheme.

Based on the constraints imposed on our mask schemes and the two components selection methods LCS and RCS, we propose three mask schemes in this paper.

Scheme (I): Enrollment Mask only with Largest Components Selection (EM-LCS). In the EM-LCS scheme, only the enrollment mask is applied. A fixed number of components are chosen based on LCS.

Scheme (II): Enrollment Mask only with Reliable Components Selection (EM-RCS). In the EM-RCS scheme, only the enrollment mask is applied. A fixed number of components are chosen based on RCS.

Scheme (III): Verification Mask only with Largest Components Selection (VM-LCS). In the VM-LCS scheme, only the verification mask is applied. A fixed number of components are chosen based on LCS. Since the enrollment mask need to be stored in the database as helper data in template protection based on the Helper Data scheme, the information from the enrollment mask may cause sensitive information leakage and lead to privacy risk. Using a verification-mask-only scheme can avoid this risk.

4. MULTI-SAMPLE FUSION OF THE SPECTRAL MINUTIAE REPRESENTATIONS

In this paper, we will investigate the strategies of fusing multiple fingerprint samples (obtained from the same sensor) at three different levels: (1) feature-level; (2) score-level; (3) decision-level, respectively. In Figure 4, we show the various processing modules of the binary spectral minutiae fingerprint recognition system, together with the stages where the feature-, score- and decision-level fusions can be performed. The output after each processing modules are: (a) minutiae set; (b) real-valued complex spectral minutiae representations; (c) the minutiae spectra after the CPCA feature reduction; (d) the Spectral Bits representation; (e) comparison scores measured by fractional Hamming Distance.

4.1 Fusion levels and their properties

For the fusion strategies at feature-, score- and decision-level, we summarize their properties in Table 1.

Information available. The information contained at the feature-level is richer than the one at the other two levels. In this sense, feature-level has the advantage.

Storage and speed requirement. When implementing score-level or decision-level fusion, all the templates derived from the multiple enrollment samples need to be stored in the database and compared with the test one during verification/identification. Therefore, the storage requirement is high and comparison (or matching) speed is slow. The feature-level fusion can be done in the enrollment stage and only a synthesized template need to be stored in the database. Therefore, the storage requirement and comparison speed will remain unchanged.

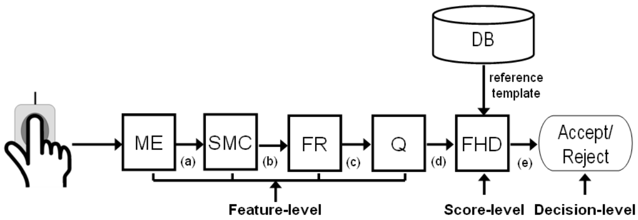

Figure 4: The various processing modules of the binary spectral minutiae fingerprint recognition system together with the stages where the feature-, score- and decision-level fusions can be performed respectively. ME: Minutiae Extractor. SMC: Complex Spectral Minutiae representation. FR: Feature Reduction. Q: Quantization. FHD: Fractional Hamming Distance.

Table 1: A summary of fusion strategies at different information level

Properties \ Level	Feature	Score	Decision
Information available	$+$	$+/-$	$-$
Storage	$+$	$-$	$-$
Speed	$+$	$-$	$-$
Ease of design	$-$	$+/-$	$+$
Template protection	$+$	$-$	$+/-$
Robustness to overfitting	$+/-$	$+$	$+$

Ease of design. Compared with the feature-level fusion, the score-level and decision-level fusion are easier to study and implement.

Template protection. As with the 'Storage' and 'Speed' properties, if multiple enrollment templates need to be stored in the database, the template protection procedure also need to be applied to each of the templates (including error correction encoding/decoding), which will greatly reduce the speed. Moreover, because of the limited error-correcting capability of error correction code, fusion at score-level with template protection also needs to be implemented differently [8].

Robustness to overfitting. The complex spectral minutiae features are complicated in relation to the amount of examples available for training the statistical model. This overfitting problem may occur during the feature-level fusion. The score- and decision-level fusions are more robust to the overfitting problem.

4.2 Feature-level fusion

During the Feature-level fusion, the features from multiple samples are combined to produce a single enrollment template. This is also known as *template consolidation* [11]. As shown in Figure 4, the feature-level fusion can be performed at the modules "Minutiae Extractor (ME)", "Complex Spectral Minutiae representation (SMC)", "Feature Reduction (FR)"and "Quantization (Q)". At each module, the amount of information available is different (the information available decreases from left to right in the figure). Fusing at minutiae feature level involves several steps such as alignment and reliable minutiae selection. Several research works have been done on this topic [6, 13]. In this paper, we will focus on the fusion of the spectral minutiae features. This can be done after the SMC, FR and Q modules. Considering the information available, implementing fusion after the SMC or FR modules is preferable over after the module Q. If we choose a linear operation for the feature-level fusion (for example, an averaging operation), implementing this fusion after the module SMC or FR is equivalent. In this paper, we will perform the spectral minutiae features fusion after the CPCA feature reduction (module FR).

In the spectral minutiae representations, the translations between fingerprint samples become invariant, while the rotations become the circular shifts in the horizontal direction. Before the feature-level fusion, we need to first align the spectral minutiae features to compensate the rotation differences. After the rotation alignment, we average the aligned spectral minutiae features to generate the synthesized enrollment (or reference) template.

Assume we have N_{E} enrollment spectral minutiae representation samples $R_1, \ldots, R_{N_{\mathrm{E}}}$ available for fusion, the procedure of our spectral minutiae feature-level fusion is as follows.

Step 1: Denote R_{i^*} as the enrollment sample with the largest similarity to all the other samples, that is,

$$i^* = \arg\max_i \sum_{\substack{k=1 \\ (k\neq i)}}^{N_{\mathrm{E}}} S^{(R_i,R_k)}, i = 1, \ldots, N_{\mathrm{E}}, \tag{5}$$

with $S^{(R_i,R_k)}$ calculated following Equation (2).

Step 2: Take R_{i^*} as the reference, align all the other enrollment samples to R_{i^*} by trying out different circular shifts following Equation (2). The aligned samples are denoted as $\widetilde{R}_1, \ldots, \widetilde{R}_{N_{\mathrm{E}}}$.

Step 3: Generate the the synthesized enrollment template R_{S} by averaging $\widetilde{R}_1, \ldots, \widetilde{R}_{N_{\mathrm{E}}}$, that is,

$$R_{\mathrm{S}} = \frac{1}{N_{\mathrm{E}}} \sum_{i=1}^{N_{\mathrm{E}}} \widetilde{R}_i. \tag{6}$$

Finally, the synthesized enrollment template R_{S} will be stored in the database as the reference template for verification/identification.

4.3 Score-level fusion

The score-level fusion is performed at the module "Fractional Hamming Distance (FHD)", see Figure 4. At this module, the binary reference templates from multiple enrollment samples are compared with the test binary template, and then multiple comparison scores are fused. The commonly used score-level fusion techniques are *Sum Rule*, *Max Rule* and *Min Rule* [15]. In Section 5, we will present the score-level fusion result based on the Max Rule[1].

4.4 Decision-level fusion

The decision-level fusion is performed at the final decision making module, see Figure 4. The very straightforward decision-level fusion techniques are *AND Rule*, *OR Rule* and *Majority Voting* [15]. The outliers in a fingerprint database can cause *false rejection*. To reduce the recognition errors caused by the outliers, in this paper, we show the performance of the decision-level fusion based on the OR Rule in Section 5[2]. It should be noted that the decision-level fusion based on the OR Rule is equivalent as the score-level fusion based on the Max Rule and their recognition performance is the same. Therefore, we will show one performance curve in Section 5.

[1]We also tried other techniques such as the Sum Rule fusion. The Max Rule fusion gives best results in our case.

[2]We also tried AND Rule and Majority Voting. The OR Rule fusion gives best results in our case.

Table 2: Permutation setting: samples used for multi-sample enrollment and single-sample verification.

Permutation	Enrollment	Genuine Verification
P1	1,2,3,4	5,6,7,8
P2	1,3,5,7	2,4,6,8
P3	1,2,7,8	3,4,5,6
P4	1,5,6,7	2,3,4,8

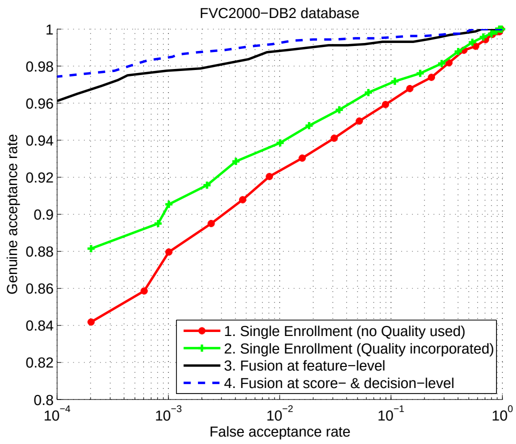

Figure 5: ROC curves of different multi-sample fusion schemes.

5. RESULTS

The proposed algorithms have been evaluated on the FVC2000-DB2 [10] fingerprint database. We apply the same experimental protocol as in the FVC competition: the samples from finger ID 101 to 110 for the CPCA training and samples from person ID 1 to 100 for test. Each identity contributes 8 samples. The minutiae sets including the minutiae quality data are extracted by a proprietary method.

We test our algorithm in a verification setting. In the single-sample enrollment case, for genuine comparisons, we used all the possible combinations. For imposter comparisons, we chose the first sample from each identity. Therefore, we generate $100 \times \binom{8}{2} = 2800$ genuine comparisons and $\binom{100}{2} = 4950$ imposter comparisons in total.

5.1 Results of Multi-Sample Fusions

To test different multi-sample fusion schemes proposed in Section 4, we set up a multi-sample enrollment and single-sample verification system. We use the Fractional Hamming Distance shown in Equation (3) as the classifier. For generating more test cases, we implemented four permutations. In each permutation, $N_{\mathrm{E}} = 4$ enrollment samples are used for multi-sample fusions and the other four samples for genuine verification. For imposter verification, we chose the first sample from each identity to compare with the multiple enrollment samples (or the synthesized enrollment template in the feature-level fusion case). The permutation setting is shown in Table 2. In total, we will generate $100 \times 4 \times 4 = 1600$ genuine comparisons and $100 \times 99 \times 4 = 39600$ imposter comparisons.

For comparison, we also present the results of the single-enrollment scheme (both with and without incorporating minutiae quality data). The ROC curves of each scheme are shown in Figure 5. From the two single-enrollment results, we can see that the recognition per-

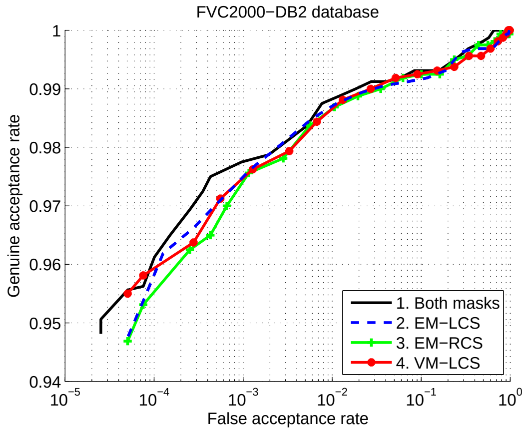

Figure 6: ROC curves of different mask schemes.

formance improved about 20% in terms of the Equal Error Rate by incorporating minutiae quality data. This improvement is consistent with the results shown in [17], where the minutiae quality data are incorporated in two other spectral minutiae representations. For the multi-sample fusion results, we can see that all the three multi-sample fusion schemes received significant improvements compared with the single-enrollment scheme. The OR Rule decision-level fusion and the Max Rule score-level fusion are equivalent and their performances are shown with one curve. They outperformed the feature-level fusion since they are more robust to outliers and the overfitting problem.

5.2 Results obtained with different Quantization Mask Schemes

The main reason to investigate the different mask schemes is for the integration of template protection schemes. As we discussed in Section 4, the feature-level fusion is most suitable for template protection schemes. In this paper, we evaluate the different mask schemes combined with the feature-level fusion algorithm. The results of four mask schemes are shown: 1. original mask schemes using both enrollment and verification masks; 2. EM-LCS; 3. EM-RCS; 4. VM-LCS. The number of masked out components are set as 5500 for EM-LCS and VM-LCS, and 5000 for EM-RCS. The ROC curves of each scheme are shown in Figure 6 (the curve of "Both masks" is the same as the "Fusion at feature-level" curve in Figure 5). We can see that the performance differences between the four schemes are not significant. For the privacy concerns as we discussed in Section 3, we recommend the VM-LCS scheme for template protection.

6. DISCUSSION AND CONCLUSION

In this paper, we investigated the multi-sample fusions of the spectral minutiae representations. We also proposed different mask schemes applied to the similarity measure of binary representations in context with template protection. Our main conclusions are: (1) Multiple enrollment samples can be used to train a statistical model of the biometric characteristics. By applying multi-sample fusions, we can obtain a more accurate representation of the biometric characteristics and improve the recognition accuracy. (2) The performance of the fusion at feature-level can be degraded due to outliers and the overfitting problem and its recognition performance can be lower than the one from score- or decision-level fusion. However, feature-level fusion has advantages on template storage requirement and comparison speed. It is also the most suitable solution when incorporating template protection. (3) When using fractional Hamming Distance, to incorporate template protection and error correction scheme, we can apply *one-mask* schemes (enrollment- or verification-mask only), which showed comparable performances as the one using both masks. (4) To prevent the sensitive information leakage, using the verification-mask-only scheme will be the best choice.

To apply the spectral minutiae representation with a template protection scheme based on the Helper Data Scheme [4], an error correction scheme is needed. Furthermore, to enhance the recognition performance, we can incorporate other fingerprint features such as singular points. Investigating the possible error correction codes and other methods to enhance recognition performance will be our future work.

7. ACKNOWLEDGMENTS

This research is supported by the ProBiTe project funding by Sentinels and the TURBINE project funding by the European Union under the Seventh Framework Programme.

8. REFERENCES

[1] ISO/IEC 19794-2, Information Technology - Biometric Data Interchange Format - Part 2: Finger Minutiae Data. 2005.

[2] J. Bringer, H. Chabanne, G. D. Cohen, B. Kindarji, and G. Zémor. Theoretical and practical boundaries of binary secure sketches. *IEEE Transactions on Information Forensics and Security*, 3(4):673–683, 2008.

[3] J. Daugman. The importance of being random: Statistical principles of iris recognition. *Pattern Recognition*, 36(2):279–291, 2003.

[4] Y. Dodis, L. Reyzin, and A. Smith. Fuzzy extractors. In P. Tuyls, B. Skoric, and T. Kevenaar, editors, *Security with Noisy Data - On Private Biometrics, Secure Key Storage and Anti-Counterfeiting*, chapter 3, pages 45–56. Springer, 2007.

[5] F. Hao, R. Anderson, and J. Daugman. Combining crypto with biometrics effectively. *IEEE Trans. Comput.*, 55(9):1081–1088, 2006.

[6] X. Jiang and W. Ser. Online fingerprint template improvement. *IEEE Trans. Pattern Anal. Mach. Intell.*, 24(8):1121–1126, 2002.

[7] A. Juels. Fuzzy commitment. In P. Tuyls, B. Skoric, and T. Kevenaar, editors, *Security with Noisy Data - On Private Biometrics, Secure Key Storage and Anti-Counterfeiting*, chapter 3, pages 45–56. Springer, 2007.

[8] E. J. C. Kelkboom, J. Breebaart, R. N. J. Veldhuis, X. Zhou, and C. Busch. Multi-Sample Fusion with Template Protection. In *BIOSIG 2009 : Proceedings of the Special Interest Group on Biometrics and Electronic Signatures.*, pages 55–67, 2009.

[9] F. J. MacWilliams and N. J. A. Sloane. *The Theory of Error-Correcting Codes (North-Holland Mathematical Library)*. North Holland, June 1988.

[10] D. Maio, D. Maltoni, R. Cappelli, J. Wayman, and A. Jain. FVC2000: Fingerprint verification competition. *IEEE Trans. PAMI*, 24(3):402–412, Mar. 2002.

[11] D. Maltoni, D. Maio, A. K. Jain, and S. Prabhakar. *Handbook of Fingerprint Recognition*. Springer Publishing Company, Incorporated, 2009.

[12] S. Prabhakar and A. K. Jain. Decision-level fusion in fingerprint verification. *Pattern Recognition*, 35:861–874, 2001.

[13] H. Ramoser, B. Wachmann, and H. Bischof. Efficient alignment of fingerprint images. In *ICPR '02: Proceedings of the 16 th International Conference on Pattern Recognition (ICPR'02) Volume 3*, page 30748, Washington, DC, USA, 2002. IEEE Computer Society.

[14] S. Raudys and A. Jain. Small sample size effects in statistical pattern recognition: Recommendations for practitioners. 13(3):252–264, March 1991.

[15] A. A. Ross, K. Nandakumar, and A. K. Jain. *Handbook of Multibiometrics (International Series on Biometrics)*. Springer-Verlag New York, Inc., Secaucus, NJ, USA, 2006.

[16] P. Tuyls, A. Akkermans, T. Kevenaar, G. Schrijen, A. Bazen, and R. Veldhuis. Practical biometric authentication with template protection. In *AVBPA*, pages 436–446, 2005.

[17] H. Xu and R. Veldhuis. Spectral minutiae representatoins of fingerprints enhanced by quality data. In *IEEE Third International Conference on Biometrics: Theory, Applications and Systems (BTAS '09)*, September 2009.

[18] H. Xu, R. Veldhuis, A. Bazen, T. Kevenaar, T. Akkermans, and B. Gokberk. Fingerprint verification using spectral minutiae representations. *Information Forensics and Security, IEEE Transactions on*, 4(3):397–409, Sept. 2009.

[19] H. Xu, R. Veldhuis, T. Kevenaar, and T. Akkermans. A fast minutiae-based fingerprint recognition system. *Systems Journal, IEEE*, 3(4):418 –427, dec. 2009.

[20] H. Xu and R. N. J. Veldhuis. Binary representations of fingerprint spectral minutiae features. In *20th International Conference on Pattern Recognition (ICPR 2010)*, Turkey, 2010. To appear.

[21] H. Xu and R. N. J. Veldhuis. Complex spectral minutiae representation for fingerprint recognition. In *Proceedings of the IEEE Computer Society Conference on Computer Vision and Pattern Recognition - Workshop on Biometrics*, San Francisco, USA, 2010.

[22] C. Yang and J. Zhou. A comparative study of combining multiple enrolled samples for fingerprint verification. *Pattern Recogn.*, 39(11):2115–2130, 2006.